Chapter 5

Forward Tracking System

5.1 Introduction

The major functions of the forward charged particle tracking system are to provide high precision momentum measurements for tracks found in the pixel system, to reconstruct and measure all parameters for tracks which do not pass through the vertex detector (such as K_s and Λ^0 daughter tracks), and to project tracks into the RICH counters, EM calorimeters, and Muon detectors. Measurements from the forward tracking system are also used online in the Level 2 trigger, as explained in Chapter 8.

5.2 General Description

The baseline forward tracking system consists of 14 stations, 7 in each arm, placed transversely to the beam at various distances from the interaction point. Three stations are placed in the fringe-field region of the dipole magnet, three stations in the field-free region just upstream of the RICH, and one station just downstream of the RICH. The entire system extends over a distance of $\sim \pm 7$ m and provides θ-angle coverage from $\sim \pm 10$ mrad up to ± 300 mrad.

The design of the forward tracking system has been driven by the high density of tracks produced in the forward direction, especially with multiple interactions per crossing. Two different types of detectors are used. Most of the solid angle is instrumented using straw tube drift chambers. Straws have been chosen because they can be used to make large chambers with small cell size, and because they can be built to surround the beam pipe without requiring a heavy frame near the beam. The track density very close to the beam requires detectors with even higher granularity; we have chosen to instrument the central section of each station with silicon microstrip detectors.

Tables 5.1 and 5.2 list all the geometric parameters and the main characteristics of the forward tracker.

This forward tracking system configuration has sufficient segmentation to handle the

Table 5.1: Properties of the baseline forward straw tracker

Property	Value
Straw size	4 mm diameter
Central hole	24 cm × 24 cm
Total Stations	14 (7 per arm)
Z positions (cm)	96, 146, 196, 296, 341, 386, 706
Half size (cm)	30, 45, 60, 90, 105, 118, 210
Views per station	3 (X,U,V)
Layers per view	3
Total number of straws	66,780
Total station thickness	0.6% X_0
Total channels	118,440
Readout	ASD + timing chip (6 bits), sparsified

Table 5.2: Properties of the baseline forward silicon tracker

Property	Value
Si-sensors	6" wafers, p-on-n type
Pitch	100 μm
Thickness	200 μm
Sensor configuration	4 ladders of 2 sensors + 2 single sensors
Coverage	24 cm × 24 cm
Central hole	5.4 cm × 5.4 cm (7 cm × 7 cm in last station)
Total stations	12 (6 per arm)
Z positions (cm)	100, 150, 200, 300, 390, 710
Views per station	3 (X, U, V)
Channels per view	3,000
Total channels	108,000
Readout	sparsified binary

high hit multiplicities that are expected when $b\bar{b}$ events are produced in the forward region. Fig. 5.1 shows occupancies in the straw tracker predicted by BTeVGeant for the case in which a $b\bar{b}$ event is produced at the design luminosity of $2{\times}10^{32}$ cm^{-2} s^{-1}. It is worth noting that these occupancies are almost a factor of two higher than those expected on average at this luminosity. The maximum occupancy in the silicon strip detectors, which have 40 times finer pitch than the straw chambers, is everywhere less than ∼4% for the conditions of Fig. 5.1.

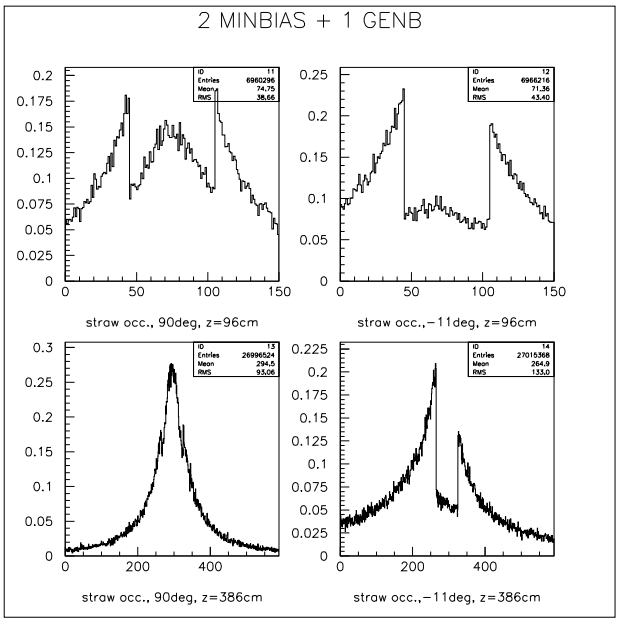

Figure 5.1: Occupancies in the first station of straws, and the station just upstream of the RICH counter, when a $b\overline{b}$ event is produced at the design luminosity of 2 $\times 10^{32}$ cm^{-2} s^{-1}. The two histograms on the left are for X-view straws, while those on the right are for U-view straws. The V-views have identical occupancies (mirrored about zero) to the U-views.

5.3 Forward Straw Tracker

5.3.1 Detector Description and Layout

The forward straw tube tracker consists of stations that provide 3 coordinate measurements, X, U and V, where the two stereo views, U and V, are at $\pm$ 11.3^o around the Y bend coordinate. With three layers per view, this configuration provides excellent resolution in the bend plane while maintaining a robust ability to reject ghost combinations of hits. It has sufficient redundancy to achieve a high detection efficiency and to resolve the left/right ambiguity a very large fraction of the time. The construction is modular, following a technique developed for the SDC straw tracker[1].

All the sense wires for the straw cells that do not terminate at the central hole are divided electrically using a small glass capillary bead following the technique used for the ATLAS TRT [2]. This cuts the occupancy rates in half. The sense wires in straws that span more than 80 cm have additional supports, which are realized following the helical design developed for the ATLAS TRT.

5.3.2 Front End Electronics and Drift Time Measurement

The straw tube chambers will be instrumented using electronics developed by the University of Pennsylvania [3], initially for the SDC straw chambers, and more recently for the ATLAS TRT. These radiation hard integrated circuits include high gain preamplifiers, pole-zero networks for pulse shaping and ion-tail cancellation, and leading edge discriminators.

The drift time will be measured using digital TDC's. The information from the straw tracker, like all information from every subsystem in the BTeV spectrometer, must be digitized and read out for every crossing. This means that a new TDC must be designed for BTeV. The small diameter of the straws makes the specifications of this TDC easy to achieve. A six-bit single-hit TDC, with 1.5 ns wide bins covering 96 ns, is sufficient to provide a drift distance measurement precision better than 100 μm.

5.3.3 Technical issues

We are developing a prototype straw tube which places an aluminum conduction layer between two Kapton films, the inner one next to the gas volume being a carbon loaded, low resistivity film. The idea is that the Kapton forms a protective barrier, similar to the graphite layers deposited on the inner surface of the ATLAS TRT straws. Without this protective barrier, there is a danger that the aluminum layer may be etched away, limiting the lifetime of the straw. We measured the surface resistivity of the aluminum coated, carbon loaded Kapton film of our prototype to be $6.5 \pm 1.0\ \Omega$/square, which is comparable to the specified value for the TRT straw tube. The details of the prototype straw material are listed in Table 5.3. The 1 mil thickness of each film is chosen as a compromise between the 0.5 mil thick films used for SDC straw tubes (which had very little mechanical rigidity) and the thicker and reinforced TRT straws. Our final design will likely have the straws supporting some of their own weight. If this turns out to not to be the case, we may use instead 0.5 mil Kapton films which have been shown to work and would provide a reduction of material in the detector volume.

Description	BTeV Straw Prototype
Kapton film	Inner: Polyimide type XC $25 \pm 2.5\ \mu m$ thickness Outer: Polyimide type 100 VN $25 \pm 2.5\ \mu m$ thickness
Density	1.42 g/cm^3
Aluminum layer	$(0.2 \pm 0.08) \mu m$ thickness
Resistivity of inner Kapton layer	$6.5 \pm 1.0\ \Omega$/square

Table 5.3: Summary of material specifications for the BTeV prototype straw tubes

5.4 Forward Silicon Tracker

5.4.1 Detector Description and Layout

Our design consists of stations with three planes of 200 μm thick single-sided silicon microstrip detectors with 100 μm pitch. On each plane, ten silicon detector wafers are mounted on low mass carbon fiber support and are arranged, wherever possible, in ladders of two daisy-chained Si-sensors to minimize the number of readout channels. The resulting configuration is depicted in Fig. 5.2.

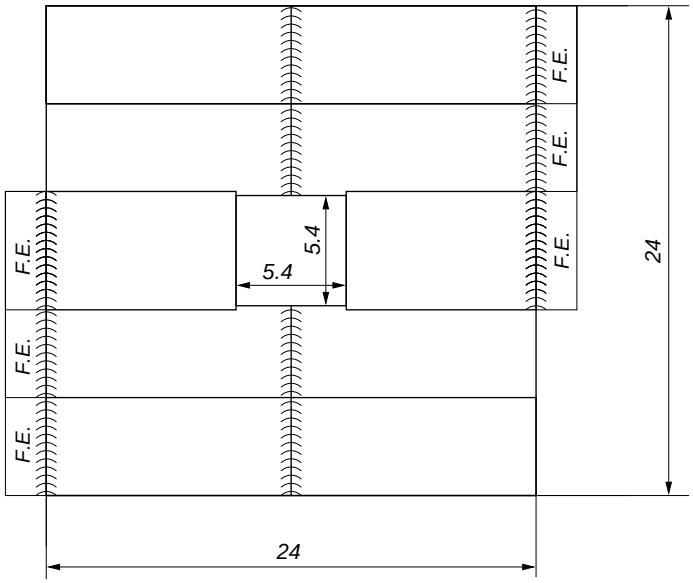

Figure 5.2: Sketch of a silicon detector plane. It consists of 4 ladders of two daisy-chained Si-sensors plus 2 single sensors. One strip overlap between contiguous detector elements ensures good efficiency over the entire plane. Dimensions are in centimeters and $F.E.$ stands for Front-End read out electronics.

Three views are provided by rotating the planes by the appropriate angles: X, U and V, where the two stereo views, U and V, are at $\pm$ 11.3^o around the Y bend coordinate. Each plane consists of about 3,000 channels; the entire system of 12 stations, 6 in each arm, has about 108,000 channels in total.

The Si-sensors, having a length up to 12 cm, are of the standard p-on-n type, with multiple n-side guard rings to allow high voltage operation, and are produced using 6" wafer technology.

The front-end electronics is distributed along the two opposite sides of each plane where it is cooled by a fluid circulating in a duct embedded in the support structure all around the periphery of the plane. This is also enough to keep the sensors at low temperature, provided that the sensors and the support are in close thermal contact. In our structure, we ensure good thermal conductivity all across the planes by employing long sensors.

The preamplifiers are AC coupled to the strips by means of capacitors directly integrated on the sensors. Each channel is read out in binary mode providing a $\sigma = 100\ \mu\text{m}/\sqrt{12} = 29\ \mu$m resolution, adequate for our physics goals.

We do not foresee any major problems in building these detectors since we can profit from the enormous experience accumulated in CDF, as well as in other experiments, and that coming from the ongoing R&D programs for LHC experiments. Nevertheless, we anticipate a possible minor concern that requires a proper backup solution. If the production of 200 μm thick 6" wafers would be problematic, we will use ladders of shorter sensors wherever necessary.

5.4.2 Radiation Issues

It is well known that the exposure of silicon detectors to high radiation doses causes damage that limits their useful lifetime. Thanks to the enormous progress accomplished during the last few years, we can now build detectors that can be operated after exposure to fluences in excess of 10^{14} particles/cm^2 [4].

In BTeV, we expect a radiation level at the silicon detectors that decreases rapidly with increasing distance from the beam. Important radiation damage effects, if any, will be confined to a small region around the central hole of the stations.

The highest levels of radiation occur at the station closest to the interaction region in the two symmetric arms of the apparatus. As shown in Fig. 5.3, the maximum value of the fluence is expected to be $\sim 1.6 \times 10^{13}$ particles/cm^2/year, given a luminosity of 2×10^{32} cm^{-2} s^{-1}. This is slightly less than the dose expected for Layer 0 of the CDF silicon tracker at the same luminosity [5]. With a proper choice of detectors, and by keeping them at low temperature, such as 0^oC, we will operate the detectors with a safety margin superior to that of CDF and those of LHC experiments. In the worst case scenario, we can expect serious radiation damage effects only on a minor portion of our detectors close to the beam after several years of operation.

We are starting an R&D program on silicon sensors to investigate other possibilities to further extend the useful lifetime of the forward silicon tracker. In particular, oxygenated sensors look very promising.

5.4.3 Readout Electronics

Even given the low occupancy expected in the Forward Silicon Tracker, the output bandwidth required to read out all hit information from every crossing is higher than is provided by any SSD chip, either already fabricated or being developed for another experiment. For this reason we have decided to develop a new readout chip with very high readout bandwidth. We will also take the opportunity to design a continuous-time-filter preamplifier capable of exploiting all the advantages offered by the relatively long bunch-crossing period of the Tevatron collider (T = 132 ns). We are considering a new preamplifier that is derived from the BaBar silicon strip front-end. We can anticipate an ENC $\sim 1000\ e^-$ for semi-Gaussian

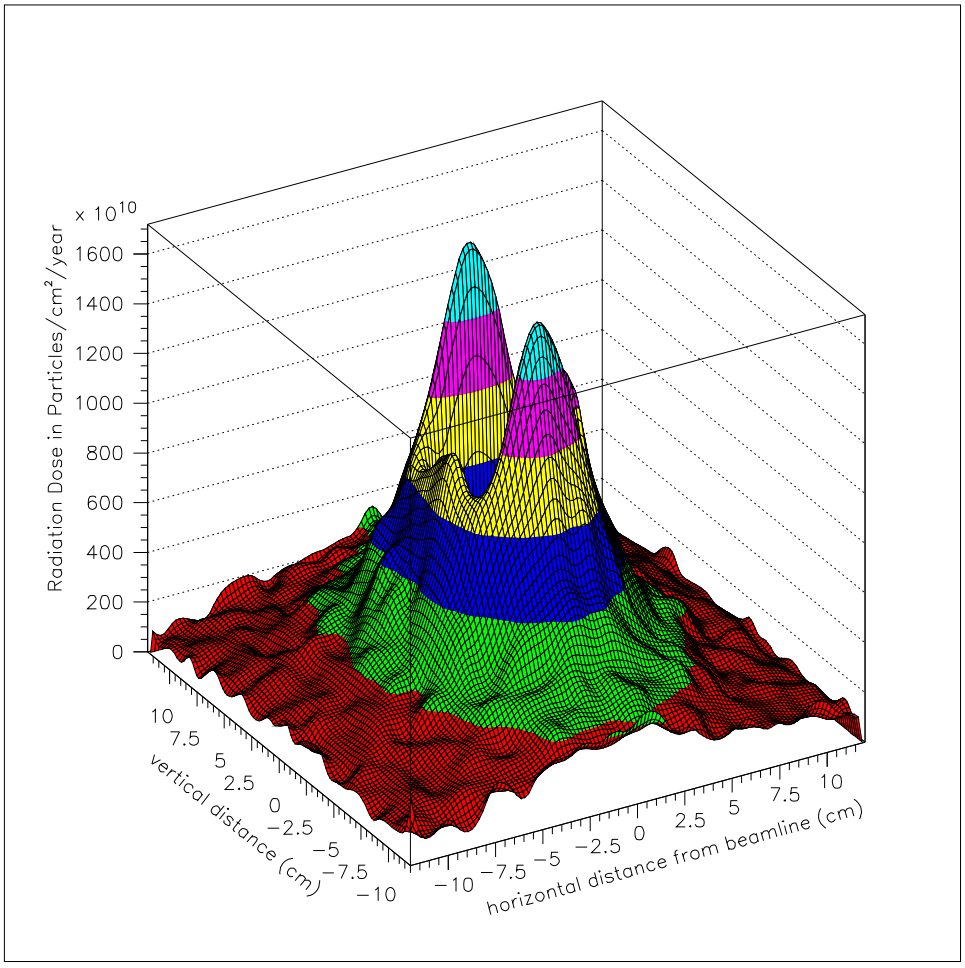

Figure 5.3: Radiation dose as a function of position in Forward Silicon Tracker Station # 1. The horizontal magnetic field concentrates more particles above and below the square central beam hole than on either side.

shaping with 100 ns peaking time and a capacitive load at the input of $\sim$30 pF, as expected for our longest strips. This noise performance represents in our view "the state of the art" for silicon strip preamplifiers.

The binary readout we are presently considering is a simplified version of the readout scheme implemented in the FPIX2 pixel readout chip. It is very fast and employs a flexible scheme for zero-suppression and readout, that can be easily adapted to strips. The SSD readout chips will be designed to interface to the same electronics we will employ to read out pixel chips.

We have initiated an R&D program to design this chip, which will be implemented using 0.25 μm CMOS, following the radiation tolerant design rules developed for the FPIX2 design.

5.5 Forward Tracker Performance

The system just described ensures excellent tracking performance over the full acceptance of the forward spectrometer. Figures 5.4 and 5.5 show the expected average fractional momentum resolution for b decay products as a function of track momentum and of the track production angle with respect to the beam axis. For these histograms, an effective position resolution of $\sigma_{X,U,V} = 150$ μm was assumed for each view of the straws and a resolution of $\sigma_{X,U,V} = 29$ μm assumed for the silicon strip detectors.

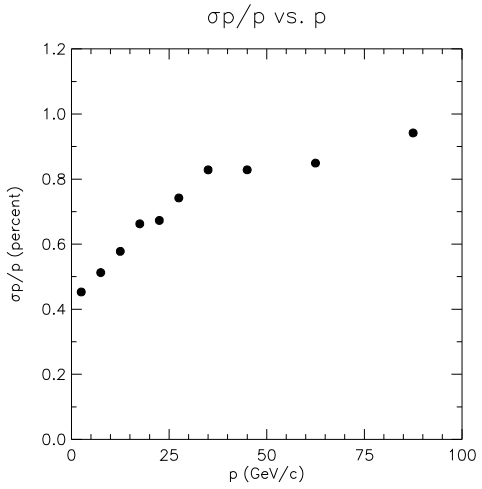

Figure 5.4: Momentum resolution as a function of track momentum for b decay products.

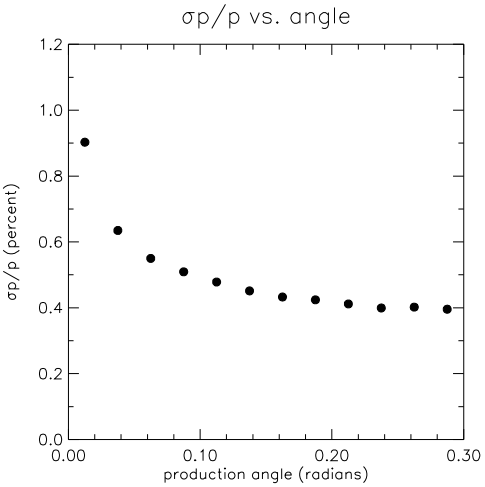

Figure 5.5: Momentum resolution as a function of polar production angle for b decay products.

Bibliography

[1] Y. Arai, *et al.*, "A modular straw drift tube tracking system for the Solenoidal Detector Collaboration experiment, Part I: Design"; Nucl. Instrum. Meth. A 381 (1996) 355.

[2] ATLAS Inner Detector Technical Design Report, CERN/LHCC/97-16,17.

[3] F.M. Newcomer, R. Van Berg, J. Van der Spiegel and H.H. Williams, Nucl. Instrum. Meth. A 283 (1989) 806.

[4] G. Tonelli, *et al.*, "The R&D program for silicon detectors in CMS"; Nucl. Instrum. Meth. A 435 (1999) 109.

[5] M.A. Frautschi, "Radiation Damage Issues for the SVX II Detector"; CDF/DOC/SEC_VTX/PUBLIC/2368.